Joule

CellPress

Preview

How Do Perovskite Solar Cells Work?

Iván Mora-Seró[1,*]

Since the first publication of all-solid perovskite solar cells (PSCs) in 2012, this technology has become probably the hottest topic in photovoltaics. Proof of this is the number of published papers and the citations that they are receiving—greater than 3,200 and 110,000, respectively— in just the last year (2017). However, despite this intensive effort, the working principles of these kind of devices are not yet fully understood. The manuscript of Ravishankar et al. will contribute significantly to this debate, as the authors have shown that the work function of the electron selecting layer plays a minor role on the final open circuit voltage, V_{oc}.

The photoconversion efficiency of a solar cell can be determined by the product of three photovoltaic parameters: photocurrent, photovoltage, and fill factor. The optimization of the photovoltaic performance requires the maximization of all three of these parameters. Although they are interrelated, each one is mostly influenced by different physical properties determining the final values. For example, maximum photocurrent is limited by the light absorbing material's bandgap, E_{gap}, but non-optimum charge collection will reduce it. As a result, establishing the working principles of each photovoltaic parameter helps not only to understand the device but to further improve its performance. However, the working principles that determine the photovoltage of perovskite solar cells (PSCs) are not as clear as those defining the photocurrent. However, these principles are not as obvious for photovoltage as for photocurrent, and the photovoltage is precisely one of the most fascinating properties of PSCs due to the high open-circuit voltage, V_{oc}, obtained with this technology.

Since the first steps of all-solid PSCs, these devices have steadily achieved remarkably high qV_{oc}/E_{gap} ratios, where q is the electron charge. In fact, the values reported for polycrystalline PSCs are one of the highest ratios (higher than 0.75[1]), only comparable with monocrystalline GaAs and GaInP.[2] Unlike photocurrent, the physical process ultimately limiting the V_{oc} of PSCs is not completely well defined and it is a topic of discussion. In fact, such debate is not new in the photovoltaic field, and it has been reproduced to some extent for each new kind of photovoltaic technology, such as sensitized or organic solar cells.

In a photovoltaic process light absorption is just the first step; it produces a splitting of the electrons and holes quasi Fermi levels E_{Fn} and E_{Fp}, respectively. The difference between these two levels is the maximum free energy available, but it can only be used to produce work after the second photovoltaic step, the charge separation. It is required to contact each quasi Fermi level independently by charge-selective contacts. Consequently, the photovoltage limit depends on the selective contacts and how the selectivity is obtained, as it can be reached by different processes[3] (see Figure 1). Figure 1A shows the band diagram of a p-i-n solar cell. In this model an intrinsic light-absorbing semiconductor is contacted by a couple of doped layers: n and p, respectively. In dark conditions with no applied bias the Fermi level, E_{F0}, equilibrates along the complete device (see Figure 1A). As the n-doped and p-doped layers present low and high work functions, respectively, the equilibration produces a built-in potential, V_{bi}. Due to the intrinsic nature of the light-absorbing layer, their bands are inclined along its complete thickness with an electrical field acting in the intrinsic region. Consequently, in this model, the contact selectivity is basically produced by the electrical field that pushes electrons and holes to n-doped and p-doped contacts, respectively. Here, the drift current plays a determinant role in charge separation and collection. The inclination of the band is affected by the applied bias and the light photocarrier generation. In fact, under illumination at open circuit, the splitting of Fermi levels produces flat band conditions (see Figure 1B) where the electrical field is removed and consequently the collection driving force cancelled, annulling the photocurrent. In this case, the V_{oc} is limited by the work functions of the contacts. This model has been used to explain the V_{oc} in amorphous Si solar cells and originally in organic solar cells.

Nevertheless, the presence of an electric field is not the only way to obtain contact selectivity. It can also be attained by a preferential kinetic exchange at one selective contact of carriers of one kind while the other kind is blocked. Figure 1C is an example of this, where light is absorbed by a dye molecule layer and electrons are selectively injected into the conduction band of a semiconductor while holes are blocked due to the band alignment. In the same way, holes are injected into a hole-transporting material. In this

[1]Institute of Advanced Materials (INAM), University Jaume I, Avenida de Vicent Sos Baynat, s/n, 12006 Castelló de la Plana, Spain

*Correspondence: sero@uji.es

https://doi.org/10.1016/j.joule.2018.03.020

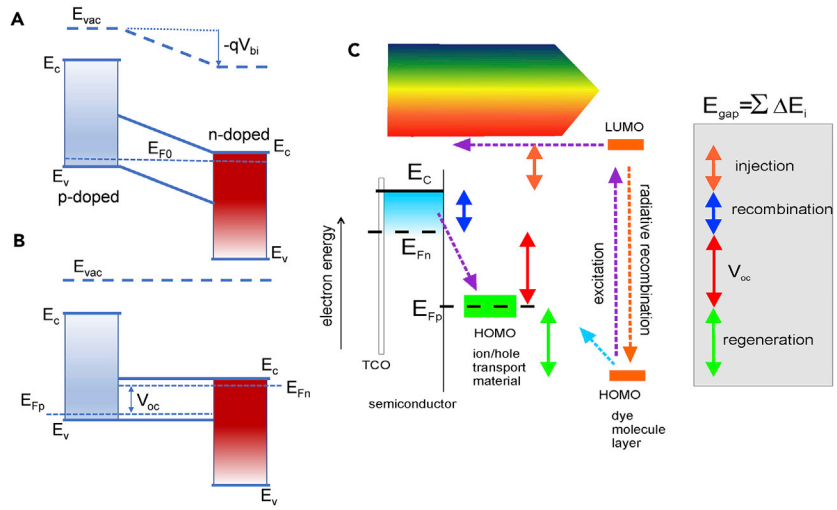

Figure 1. Band Diagrams of Electric Field and Diffusion-Driven Solar Cells

(A and B) Energy band diagram at open circuit conditions for a p-i-n solar cell (A) under dark and (B) under illumination.[4] E_{vac}, E_C, E_V, E_{F0}, E_{Fn}, and E_{Fp}, are the vacuum, the conduction band, the valence band, the Fermi equilibrium, the quasi Fermi for electrons, and the quasi Fermi for holes energy levels, respectively; q is the electron charge, and V_{bi} is the built-in potential.

(C) Energy diagram of dye-sensitized solar cells, where a dye is acting as light-absorbing material. Photogenerated electrons are injected into a semiconductor, generally TiO_2, performing as an electron transporting layer and extracted through a transparent conducting oxide (TCO). Dye is regenerated by a hole-transporting material. The different energy losses making the V_{oc} sensibly lower than E_{gap} are indicated. Figure 1C is reproduced with permission from RSC.[5]

case, as is indicated in Figure 1C, the V_{oc} is limited by the difference of quasi Fermi levels at the electron and hole-selective contacts. Here, the difference of work functions is absorbed in thin interfacial layers, such as the transparent conduction oxide/TiO_2 interface in the particular case of sensitized solar cells. In fact, Si solar cells have a similar selectivity mechanism where the band bending produced by the p-n junction is limited to a very narrow interfacial layer, significantly thin in comparison with the whole absorber thickness. There are also intermediate models between those two noted in Figure 1. It is the case of CIGS solar cells, where the band bending region of p-n junction is thinner than the total thickness, but it is not as thin as the example depicted in Figure 1C.[3]

In the early days of dye-sensitized solar cells, there was intense debate about the photovoltage-determining mechanism in these kinds of cells, between the two models presented in Figure 1. Pichot and Gregg finally demonstrated that it is the model presented in Figure 1C that rules sensitized devices.[6] They deposited dye-sensitized TiO_2 films on four different substrates that have vacuum work functions spanning a 1.4 eV range and measured the obtained photovoltage in three different redox electrolyte solutions, observing no significant differences.

It seems quite obvious to follow the same procedure as Pichot and Gregg to determine the working mechanisms of perovskite solar cells, but it is not straightforward at all. A number of published works vary the work function of the contacts in PSCs with a broad dispersion of results; some of these reports show certain voltage dependence on the work function, while others present no dependence, or even no clear trends. Some examples of these studies have been recently reviewed.[7] This dispersion of results lies in the fact that contacts influence the perovskite layer itself, hampering a fair comparison among PSCs prepared with different contacts. In sensitized solar cells, in contrast, it was very easy to replace one part of the cell, keeping the other parts invariant. In the case of PSCs, the nucleation and crystal growth processes of the perovskite layer are influenced by the contact in which the perovskite is deposited, even if the same deposition procedure is employed. In this sense, it is difficult to decouple the effect of the contact and the effect of the change of morphology. Moreover, the deposition of the contact onto the absorber could also influence the upper part of the perovskite layer; and those changes, even in a very thin region of the perovskite interface, can produce significant effects.[8]

One of the biggest challenges in the manuscript of Ravishankar et al. has been the fabrication of the state-of-the-art PSCs with electron-selecting contacts with work functions away from more than 1 eV, with very similar thickness, morphology, light absorption, and crystallinity, thus allowing a fair comparison.[9] Despite this huge difference in work functions, they observed very similar V_{oc}, pointing to a minor role of the built-in electrical field. In contrast, V_{oc} is generated by the Fermi level splitting at the perovskite layer, where each selective contact follows the quasi Fermi level of the respective carrier in the perovskite layer. This fact has very important consequences in the working principles of PSCs as quasi Fermi level splitting and consequently V_{oc} is controlled by light absorption and carrier recombination (see Figure 1C). If electrical fields are not playing a major role, mostly flat bands should be expected in the perovskite layer with transport dominated by diffusion. If the selective contact follows the Fermi level of the perovskite and is influenced by the perovskite layer, they should not be treated as a mere series of connected systems but as parallel interrelated layers, a fact that could influence, for example, future impedance models of the device. Further research and experiments will be needed to confirm, modify, and complete

this model, but the work of Ravishankar et al. undoubtedly constitutes a valuable piece of work aiming to determine the working principles of perovskite solar cells.

1. Anaraki, E.H., Kermanpur, A., Steier, L., Domanski, K., Matsui, T., Tress, W., Saliba, M., Abate, A., Gratzel, M., Hagfeldt, A., and Correa-Baena, J.-P. (2016). Highly efficient and stable planar perovskite solar cells by solution-processed tin oxide. Energy Environ. Sci. *9*, 3128–3134.

2. Nayak, P.K., and Cahen, D. (2014). Updated assessment of possibilities and limits for solar cells. Adv. Mater. *26*, 1622–1628.

3. Kirchartz, T., Bisquert, J., Mora-Sero, I., and Garcia-Belmonte, G. (2015). Classification of solar cells according to mechanisms of charge separation and charge collection. Phys. Chem. Chem. Phys. *17*, 4007–4014.

4. Bisquert, J. (2017). The Physics of Solar Cells: Perovskites, Organics, and Photovoltaic Fundamentals (CRC Press), p. 81.

5. Barea, E.M., Ortiz, J., Pay, F.J., Fernádez-Lázaro, F., Fabregat-Santiago, F., Sastre-Santos, A., and Bisquert, J. (2010). Energetic Factors Governing Injection, Regeneration and Recombination in Dye Solar Cells with Phthalocyanine Sensitizers. Energy Environ. Sci. *3*, 1985–1994.

6. Pichot, F., and Gregg, B.A. (2000). The photovoltage-determining mechanism in dye-sensitized solar cells. J. Phys. Chem. B *104*, 6–10.

7. Fakharuddin, A., Schmidt-Mende, L., Garcia-Belmonte, G., Jose, R., and Mora-Sero, I. (2017). Interfaces in Perovskite Solar Cells. Advanced Energy Materials, 1700623-n/a.

8. Will, J., Hou, Y., Scheiner, S., Pinkert, U., Hermes, I.M., Weber, S.A.L., Hirsch, A., Halik, M., Brabec, C., and Unruh, T. (2018). Evidence of tailoring the interfacial chemical composition in normal structure hybrid organohalide perovskites by a self-assembled monolayer. ACS Appl. Mater. Interfaces *10*, 5511–5518.

9. Ravishankar, S., Gharibzadeh, S., Roldán-Carmona, C., Grancini, G., Lee, Y., Ralaiarisoa, M., Asiri, A.M., Koch, N., Bisquert, J., and Nazeeruddin, M.K. (2018). Joule *2*, this issue, 788–798.

Preview

Electrochemical CO_2 Reduction via Low-Valent Nickel Single-Atom Catalyst

Jingguang G. Chen[1,*]

Electrochemical conversion of CO_2 to CO with high intrinsic activity, selectivity, and stability was demonstrated on a low-valent Ni single-atom catalyst. The nature of catalytic sites and their evolutions under catalytic condition were identified, which should provide important guidance toward building efficient electrocatalysts for CO_2 reduction.

Atomically dispersing metal atoms on supports provides an ideal strategy for maximizing metal utilization for catalysis, which is particularly important for fabricating cost-effective catalysts based on Earth-scarce metals. Electrochemical CO_2 reduction to chemical feedstocks and fuels presents a promising strategy for managing the global carbon balance, but with the greatest challenges being the lack of efficient and durable electrocatalysts.[1] Inorganic candidates such as Au, Ag, and Cu have been widely investigated.[2–4] However, they generally suffer from large overpotential, insufficient faradaic efficiency, and poor durability; thus, it is still a long-term goal to realize their practical applications. A single-atom catalyst with atomically distributed active metal center has recently been explored as a bridge to link between heterogeneous and homogeneous catalysis, which has attracted intense research interests in electrochemical reactions. Such an approach provides a useful strategy to maximize the metal utilization, which is particularly important for cost-effective catalysts based on scarce metals. Moreover, the single-atom catalyst also has unique structural and electronic properties that can be tuned by the coordination environment.[5,6]

Recently, Huang, Zhang, Liu, and co-workers[7] reported excellent performance of a single-Ni-atom catalyst for CO_2 electrochemical reduction. The newly developed single-Ni-atom catalyst exhibits unprecedented intrinsic CO_2 reduction activity, achieving a specific current of 350 A $g_{catalyst}^{-1}$ and TOF of 14,800 h^{-1} at a mild overpotential of only 0.61 V for CO conversion with 97% faradaic efficiency. The catalyst also maintains 98% of its initial activity after 100 hr of continuous reaction with CO formation current density as high as 22 mA cm^{-2} (55 mA $mg_{catalyst}^{-1}$).

The single-Ni-atom catalyst was prepared by a simple two-stage (600°C and 900°C) pyrolyzation of melamine, nickel acetate, and an amino acid in argon, and the process could be easily scalable. During pyrolysis, melamine underwent poly-condensation in the temperature range of 370°C–600°C to form defective graphitic carbon nitride (g-C_3N_4),[8] and at the same period the nickel(II) atoms were immobilized onto the defect sites of g-C_3N_4 by the amine

[1]Department of Chemical Engineering, Columbia University, New York, NY 10027, USA

*Correspondence: jgchen@columbia.edu

https://doi.org/10.1016/j.joule.2018.03.018